We are IntechOpen,
the world's leading publisher of
Open Access books
Built by scientists, for scientists

4,800
Open access books available

122,000
International authors and editors

135M
Downloads

Our authors are among the

154
Countries delivered to

TOP 1%
most cited scientists

12.2%
Contributors from top 500 universities

CLARIVATE ANALYTICS
BOOK CITATION INDEX
INDEXED

WEB OF SCIENCE™

Selection of our books indexed in the Book Citation Index
in Web of Science™ Core Collection (BKCI)

Interested in publishing with us?
Contact book.department@intechopen.com

Electrospun Metal Oxide Nanofibers and Their Energy Applications

Yingjie Liao, Takeshi Fukuda and Suxiao Wang

Additional information is available at the end of the chapter

Abstract

Metal oxide nanofibers have attracted considerable research interest for processing both one-dimensional nanometer scale morphology and unique chemical and electrical properties. A variety of their practical applications in light-emitting diodes, liquid crystal displays, solar cells, and gas sensors have been demonstrated. Electrospinning provides a rapid and facile way to fabricate nanofibers with diameter several orders of magnitude smaller than that produced by conventional spinning methods. In this chapter, we discuss the fabrication of ultrathin metal oxide nanofibers by the electrospinning technique. Priority is given to zinc oxide nanofibers. Major parameters affecting the morphology and diameter of the nanofibers are investigated systematically. The effect of calcination condition on chemical composition and crystallization of the electrospun nanofibers is also addressed. In addition, we show the advantages and problems when applying electrospun nanofibers to solar cells.

Keywords: electrospinning, metal oxide nanofibers, solar cells, energy, zinc oxides

1. Introduction

Nanofibers have been widely used in many areas, including catalysis [1–3], tissue engineering [4–7], filtration [8–10], biomedical [11–13], sensors [14–16], energy [17–19], and magnetic [20, 21]. The most common ceramic materials of nanofibers are zinc oxide (ZnO), titanium dioxide, silicon dioxide, zirconium dioxide, aluminium oxide, and lithium titanate [22–24]. Nanofibers can be synthesized by various methods, such as melting processing, antisolvent-induced polymer precipitation, electrospinning, island in the sea, or direct drawing from a solution [25–27]. Electrospinning is one of the mostly studied techniques due to its simplicity

of experimental setup and relatively high production rate. As shown in **Figure 1**, the number of published papers on electrospun nanofibers every year increases quickly in the past 10 years.
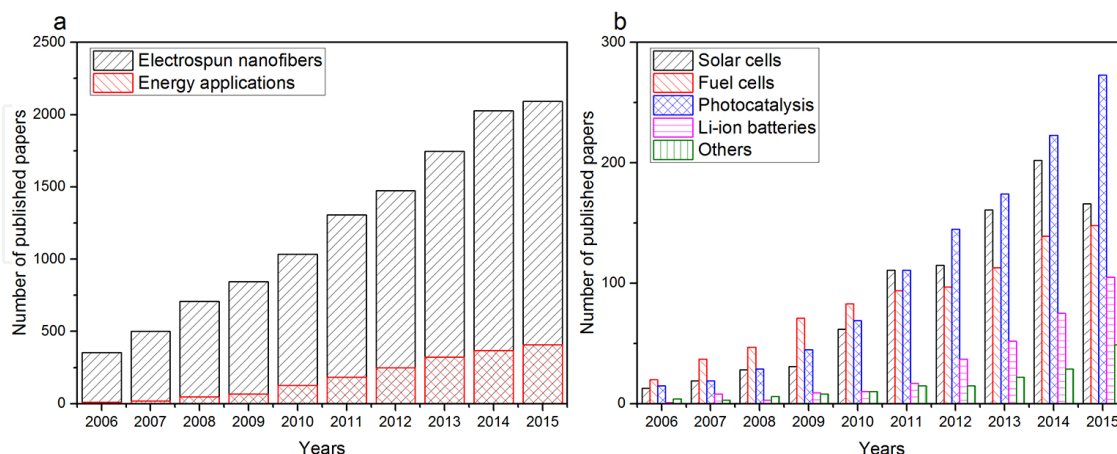

Figure 1. Comparison of the number of research publications (a) on electrospun nanofibers and their energy applications part and (b) on major energy applications of nanofibers in the past 10 years. The data are obtained from Web of Science Core Collection.

As the demand for energy is growing rapidly in recent years, energy conversion and energy storage become hot research topics. Nanofibers and other one-dimensional structures, such as nanowires, nanorods, nanobelts, and nanotubes, have been investigated intensively for their unique properties in energy applications [28–31]. As indicated in **Figure 1a**, about 20% of publications on electrospun nanofibers are for energy applications in 2015. Nanofibers, especially metal oxide nanofibers, possess unique optical and electrical characteristics and have been used in various energy devises [2, 32]. The number of published research articles on the energy application of nanofibers shows exponential increment in the past 10 years. Most of them focus on solar cells, fuel cells, lithium ion batteries, and photocatalysis applications. Other applications, e.g., super capacitors and hydrogen generation, are also attracted a lot of research interest.

In this chapter, we introduce the electrospinning technique briefly and discuss the processing parameters for controlling the diameter and morphology of electrospun metal oxide nanofibers as exemplified by ZnO nanofibers. Then, we show applications of nanofibers in energy conversion (e.g., energy devices and fuel cells) and energy storage (e.g., lithium ion batteries) and figure out the challenges for these applications.

2. Electrospinning of ultrathin metal oxide nanofibers

2.1. Electrospinning technique

The electrospinning technique is considered as one of the most simple and effective ways to fabricate nanofibers. **Figure 2** shows a schematic diagram of an electrospinning setup. A basic

electrospinning setup usually consists of three parts: a high-voltage power supply, a spinneret, and a collector. To facilitate monitoring the state of the electrospinning, a laser and a CCD camera are sometimes added into the setup. The inset of **Figure 2** is obtained from a CCD camera and illustrates a typical image of a spinning jet during the electrospinning. A common high-voltage power supply for electrospinning is a direct current power in the range of several kV to about 20 kV. The spinneret is usually connected with a syringe to hold more solution and control the flow rate. The inner diameter of the spinneret can be smaller and more individual for glass capillaries compared to metallic needles. The collector could be an aluminium foil or other substrates with conductive surface, which depends on practical application.
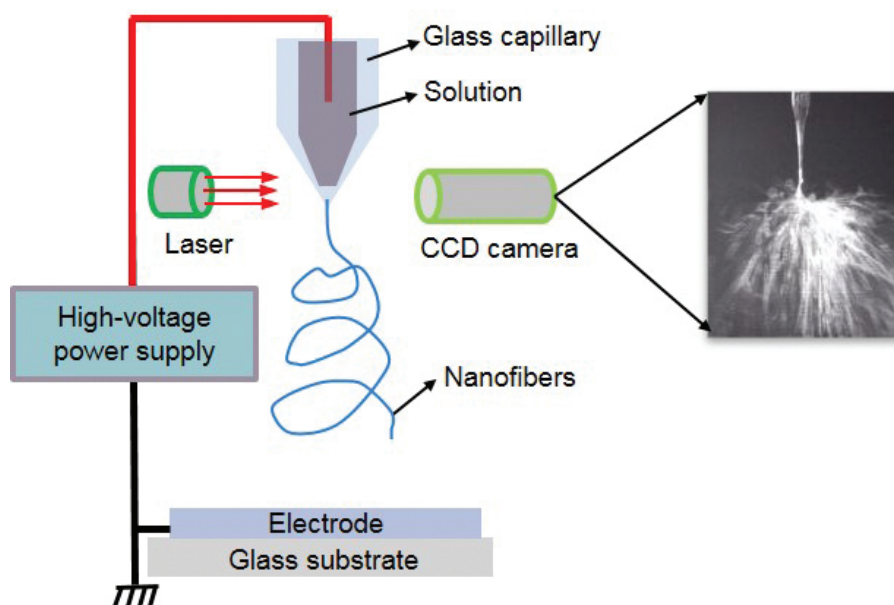

Figure 2. A schematic diagram of the electrospinning apparatus. Inset shows the CCD image of electrospinning process near the tip of the glass capillary.

The electrospinning setup is rather simple and can be built easily, however, the mechanism of electrospinning is very complicated [18, 27]. When a high voltage is applied to the liquid inside the spinneret, an electrical filed is set up between the spinneret and the collector. The liquid (usually a polymer solution) reaching the spinneret tip forms a Taylor cone, which emits a liquid jet through its apex. This electrified liquid jet undergoes a stretching and whipping process, which leads to the formation of a long and thin thread. As the liquid jet is continuously elongated and the solvent is evaporated, its diameter can be greatly reduced from hundreds of micrometres to as small as tens of nanometres. Attracted by the grounded collector placed under the spinneret, randomly orientated fibres are deposited [24].

Nanofibers with novel structures can be archived by modifying the basic electrospinning setup in a number of ways. Modifications are usually in the spinneret or the collector. It has been demonstrated that a spinneret containing two needles could be used to electrospun composite nanofibers. In another approach, a spinneret consisting of two coaxial capillaries has been

used to fabricate fibres with core/sheath or hollow structures. In addition, the orientation of electrospun nanofibers can be controlled by changing the electrode of the collector. One also can get relatively uniform mat by replacing the planar collector with a rotating drum.

2.2. Controlling the diameter and morphology of electrospun nanofibers

The diameter and morphology of electrospun nanofibers are two key factors, which should be controlled for practical applications. They are dependent on a lot of processing parameters relevant to the solution and setup conditions. The intrinsic properties of the solution play important role in determining the diameter and morphology of resultant nanofibers. One can get target nanofibers by changing the type of the polymer, the conformation of polymer chain, or by adjusting concentration, viscosity, elasticity, electrical conductivity, and the polarity and surface tension of the solution. The conditions of electrospinning setup, e.g., the flow rate for the solution, the applied voltage, the distance between the spinneret and the collector, could also affect tremendously the diameter and the morphology of electrospun nanofibers. In addition to these parameters, variables of evaporation, such as temperature and humidity, may also influence the two key factors.
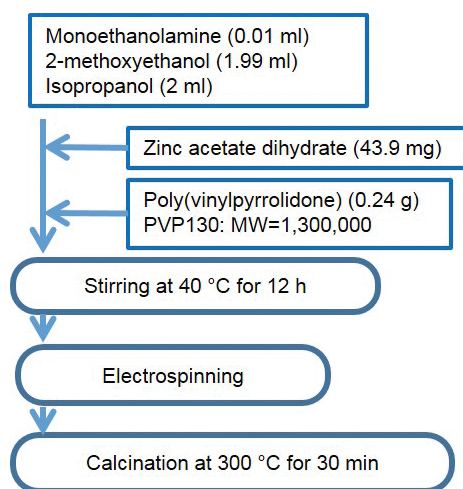

Figure 3. A typical procedure for preparing the ZnO nanofibers by electrospinning.

Here, we take the electrospinning of ZnO nanofibers as an example to explain how to control the diameter and morphology of electrospun nanofibers. **Figure 3** shows a typical procedure for the electrospinning of ZnO nanofibers. In this progress, 43.9 mg of $Zn(CH_3COO)_2 \cdot 2H_2O$ (zinc acetate dihydrate) was first dissolved in a monoethanolamine (MEA)-2-methoxyethanol solution at room temperature. The molar ratio of MEA to zinc acetate dihydrate was kept at 1.0, and the concentration of zinc acetate was 0.1 mol/L. The resultant mixture was stirred at 40°C for 12 hours to obtain a transparent and homogeneous solution. Then polyvinylpyrrolidone (PVP) was added into the ZnO sol-gel solution to increase the viscosity of the solution. The solution was finally loaded into a glass capillary with a 100 μm inner diameter at the blunt tip. A stable high voltage of 6.0 kV was generated by a high-voltage power supply and was applied to the solution through a copper wire in the glass capillary. In addition, an indium tin

oxide (ITO)–coated glass substrate (25 mm × 25 mm) was placed perpendicular to the axis of the capillary at a distance of 10 cm from its tip as a collector for solar cell applications (see next section). The collector was connected to the ground along with the high-voltage power supply. The effect of three processing parameters relevant to the properties of the precursor solution, molecular weight of PVP, the concentrations of zinc acetate and PVP in the precursor solution, on the diameter and morphology of electrospun ZnO nanofibers is investigated systematically.

2.2.1. Effect of the concentration of precursor solution

SEM images in **Figure 4** show the progression of ZnO-PVP composite from grains to nanofibers when the concentration of PVP in the precursor solution increases from 0.02 to 0.06 g/mL. It is rather clear that only ZnO-PVP composite grains with various sizes are formed with 0.02 g/ml PVP regardless of the concentration of zinc acetate. This implies that the electrospun product is grains instead of nanofibers when the PVP in the solution could not provide enough viscosity for electrospinning.
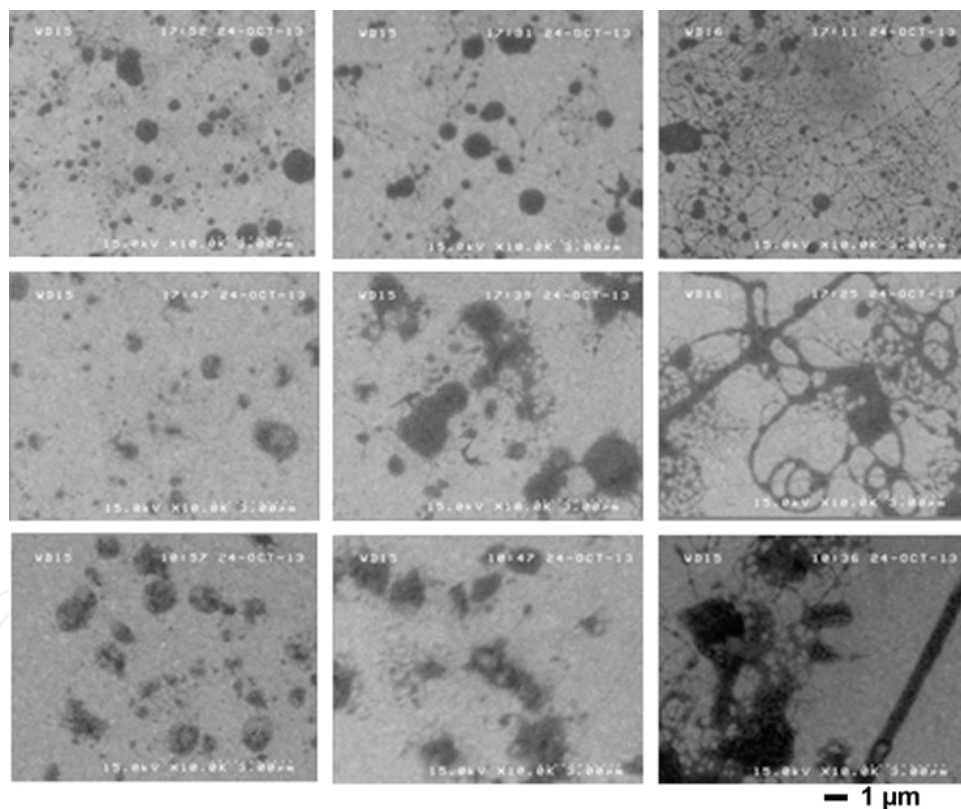

Figure 4. SEM images of the ZnO-PVP composite structure electrospun from a mixture of ZnO sol-gel and PVP solution. Concentrations of zinc acetate are 0.1 M (top row), 0.4 M (middle row), and 0.75 M (bottom row); those of the PVP solution are 0.02, 0.04, and 0.06 g/mL from the left to the right column, respectively [33].

As the concentration of PVP is increased to 0.04 g/mL, a few ZnO-PVP nanofibers appear among ZnO-PVP grains, see the middle column of **Figure 4**. When the concentration of PVP reaches 0.06 g/mL, ZnO-PVP nanofibers become predominant (right column of **Figure 4**). It is

worth noting that similar progression from grains to nanofibers is taken place in all solutions (0.1 M, 0.4 M and 0.75 M zinc acetate). So, we can conclude that it is not the concentration of zinc acetate but the concentration of PVP, which determines the formation of ZnO-PVP nanofibers.
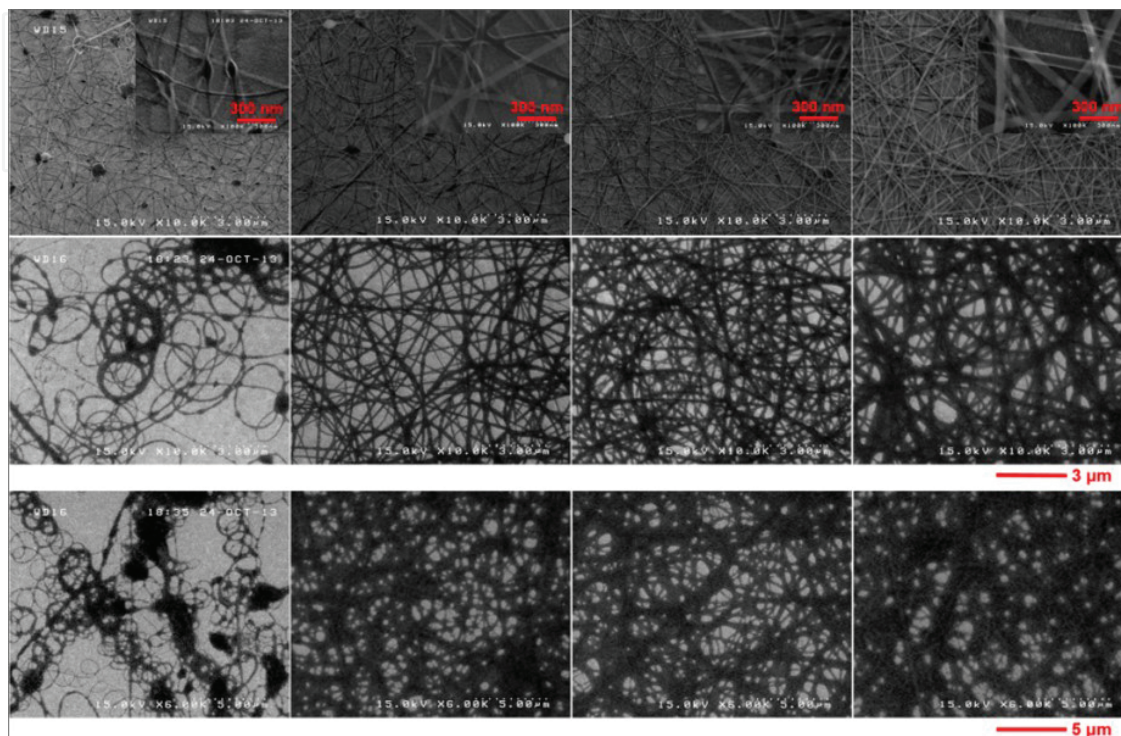

Figure 5. SEM images of the ZnO-PVP composite nanofibers electrospun from a mixture of ZnO sol–gel and PVP solution. Concentrations of zinc acetate are 0.1 M (top row), 0.4 M (middle row), and 0.75 M (bottom row); those of the PVP solution are 0.06, 0.08, 0.12, and 0.14 g/mL from the left to the right column, respectively. High-magnification SEM images are shown as insets [33].

SEM images in **Figure 5** show the effect of the concentration of precursor solution on the diameter of the ZnO-PVP composite nanofibers. One can see that the diameter of electrospun nanofibers increases steadily with the concentration of PVP for all three groups of samples. And the beads present in the top row images (0.1 M zinc acetate) become less prominent with the growth of the nanofibers, which can also be attributed to the increment of the viscosity of the precursor solution induced by more PVP [27]. These results suggest that the concentration of PVP in the precursor solution plays a significant role in determining not only the size of the nanofibers but also the absence of the beads. As for the concentration of zinc acetate, we find that it could also influence the diameter of resultant nanofibers when comparing the three groups of samples in **Figure 5**. Relatively high molar concentration of zinc acetate induces the formation of thicker ZnO-PVP composite nanofibers. Moreover, the nanofibers synthesized with 0.1 M zinc acetate are more uniform than those in the other two groups. In general, the diameter of ZnO-PVP nanofibers can be controlled through changing the concentration of either PVP or zinc acetate in the precursor solution. But thin ZnO-PVP

nanofibers are produced commonly with some beads at low concentration of the precursor solution.

In order to analyze quantitatively and compare the effect of the concentration of PVP and zinc acetate on the size of the resultant nanofibers, we measured the diameter of the nanofibers from their high-resolution SEM images and plotted the mean of 50 measurements with corresponding standard error for each sample (**Figure 6**).
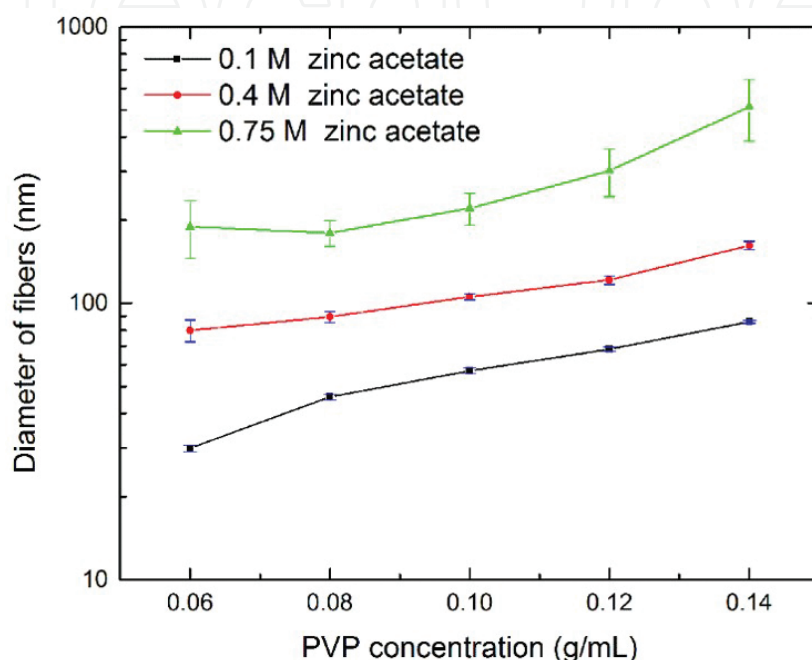

Figure 6. Statistics for the diameter of the ZnO-PVP nanofibers [33].

For the ZnO nanofibers synthesized with 0.1 M zinc acetate, their diameter increase almost linearly with the concentration of PVP. The finest ZnO nanofiber is 29.9 ± 0.8 nm in diameter. In the case of 0.4 M zinc acetate, the diameter of electrospun ZnO nanofibers increased superlinearly from 79.9 ± 7.1 to 162.0 ± 5.5 nm as the PVP concentration increased from 0.06 to 0.14 g/mL. Comparing the fibres synthesized with given PVP concentration, we found that their diameter increases considerably with the molar concentration of zinc acetate. We also noticed that the standard error of the mean diameter for the fibres synthesized with 0.4 and 0.75 M zinc acetate, especially the latter, is larger than the case of 0.1 M zinc acetate, which implies that the concentrated ZnO sol-gel solution disturbed the balance electrospinning set up by the PVP component. In general, one can get ZnO nanofibers with large diameter by increasing the concentration of zinc acetate or PVP in the precursor solution. And the former could contribute to greater nonuniformity in the distribution of the diameter than the latter.

2.2.2. Effect of the molar mass of polymer and applied voltage

As indicated by the Mark-Houwink equation, the intrinsic viscosity of a polymer is related to its molecular weight. That means one can adjust the viscosity of a polymer solution by

changing the molar mass of the polymer. The parameters of electrospinning setup could also influence the diameter and morphology of electrospun nanofibers. Here, the molar mass of PVP and applied voltage are investigated together.
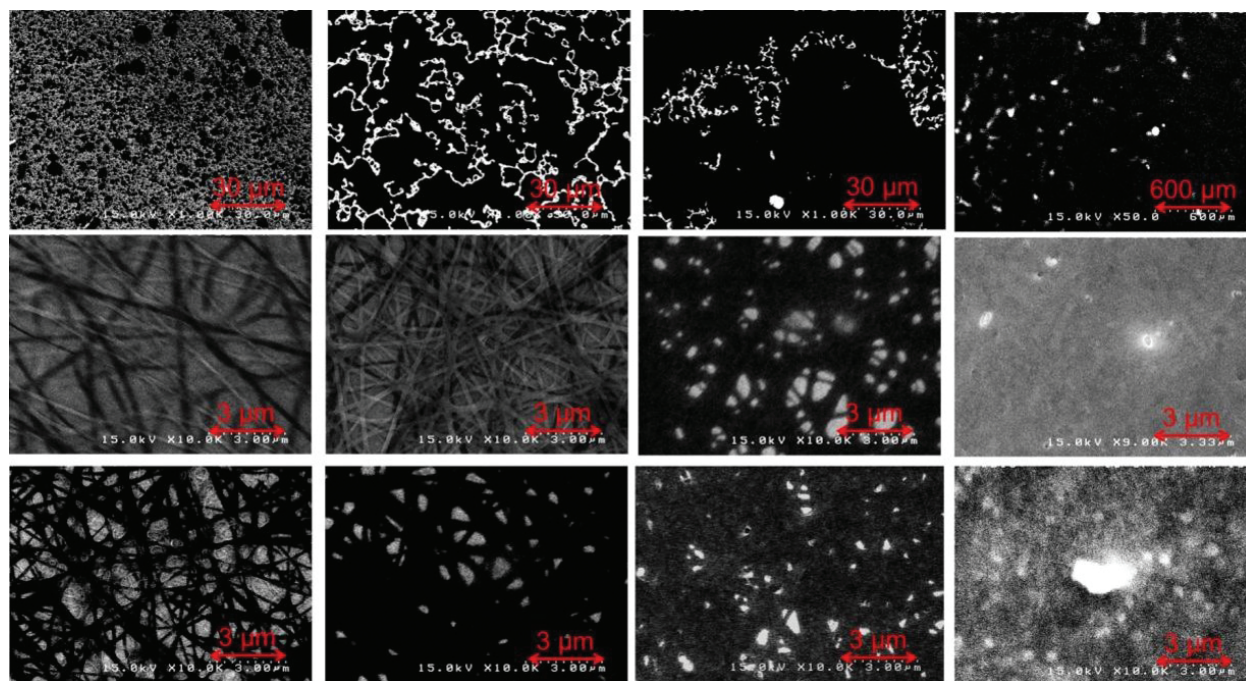

Figure 7. SEM images of ZnO-PVP nanofibers electrospun with PVP of different molar mass (top: 40,000; middle: 360,000; bottom: 1,300,000). And the high voltage applied to the spinneret is 6, 7, and 8 kV from left to right.

One can see from the first row in **Figure 7**, with PVP 40,000, the electrospun product is varicose fibres with relative large size and short length. As the applied voltage increases from 6 to 8 kV, the size of fibres become larger, but the amount of fibres is fewer. For PVP 360,000 and PVP 1,300,000, ZnO-PVP nanofibers are observed. These nanofibers get denser with increment of the applied voltage. On the whole, the role of the molar mass of PVP in determining the diameter of ZnO-PVP nanofibers is similar to that of the concentration of precursor solution. At the same time, turning the concentration is much easier than changing the molar mass for practical application. The applied voltage could also affect the size of electrospun nanofibers, but not as direct as other parameters discussed above.

2.3. Crystallization of metal oxide nanofibers

Electrospinning of composite nanofibers is the first step for the preparation of metal oxide nanofibers. In order to improve the purity and other characteristics of the composite nanofibers (e.g., transmittance, mobility, and crystallinity) for energy application, calcination will be conducted after electrospinning. For example, the as-spun ZnO-PVP nanofibers described above could be subsequently converted into ZnO nanofibers with pure phase through calcination. In this section, we discuss the calcination conditions for the crystallization of metal oxide nanofibers.
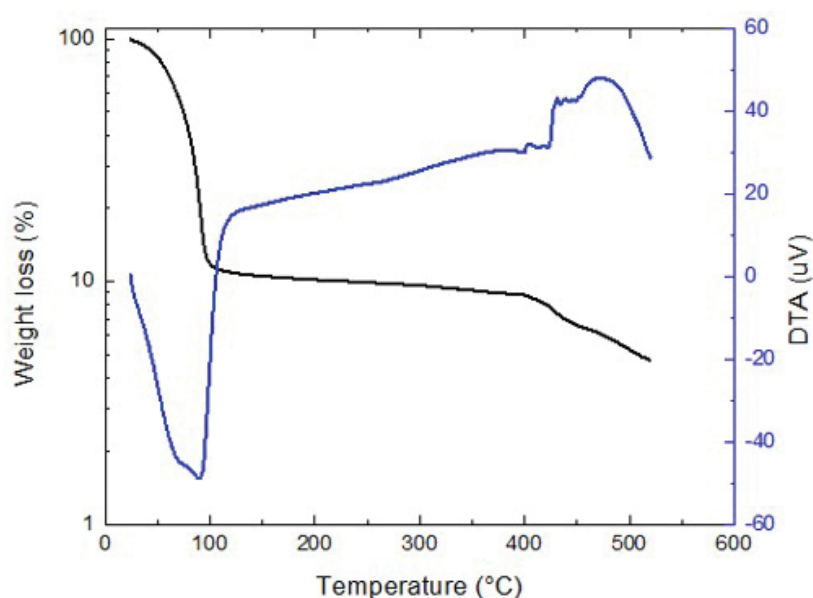
Figure 8. Thermogravimetric analysis curves of as-spun ZnO-PVP nanofibers.

To determine the decomposition temperature of the precursor and the calcination tempera-
ture for the ZnO-PVP nanofibers, thermogravimetric analysis for the as-spun ZnO-PVP
nanofibers was performed and shown in **Figure 8**. For the thermogravimetric analysis curve,
the residue weight of the as-spun ZnO-PVP nanofibers is only 4.73%. Most organic in the as-
spun ZnO-PVP nanofibers comes from PVP, and the CH_3COOH group of zinc acetate was
removed at a temperature below 480°C. A strong endothermic peak appeared at around
100°C in the differential thermal analysis (DTA) curve, which corresponds to the loss of
absorbed water. The exothermic peak at around 400, 430, and 463°C in the DTA curve may
have resulted from decomposition on the side and main chains of PVP. The thermogravimet-
ric analysis indicates that a calcination temperature of the as-spun ZnO-PVP nanofibers may
existed above 480°C.

Transmission electron microscopy (TEM) images in **Figure 9** show the microscopic structure
of ZnO nanofibers after calcination under different conditions. The diameter of as-spun ZnO-
PVP nanofibers is around 120 nm before calcination. After calcination at 300°C for 10 mi-
nutes, the diameter of the nanofibers does not change a lot, see **Figure 9a**. And the shape of
the nanofibers is rather uniform. Even from the magnified image of **Figure 9a** (see **Figure 9b**),
it is difficult to identify ZnO grains, which suggests that the ZnO did not crystallize suffi-
ciently. From the thermogravimetric analysis above, one can know that the PVP component
in the as-spun ZnO nanofibers did not decompose at 300°C. This means that the as-spun ZnO-
PVP nanofibers need higher calcination temperature and longer calcination duration to
remove the PVP content and crystallize as-spun ZnO-PVP nanofibers. **Figure 9c** shows the
TEM image of the as-spun ZnO-PVP nanofibers calcined at 500°C for 2 hours. The diameter
of the nanofiber shrinks down to about 50 nm. It is clear that the nanofiber is composed of
many single isolated ZnO grains. The lattice images of ZnO in **Figure 9d** suggest that ZnO
crystallized under this calcination condition, which is also evidenced by the X-ray diffrac-

tion (XRD) analysis given below. The growth direction of the crystalline ZnO is indicated by a red arrow in **Figure 9d**. By comparing the two samples of ZnO-PVP nanofiber calcined under different conditions, one can learn that as-spun ZnO-PVP nanofibers could be converted into crystallized ZnO nanofibers by calcination at 500°C for 2 hours in air. Calcination at 300°C for 10 minutes is insufficient for the decomposition of PVP and crystallization of ZnO-PVP composite.
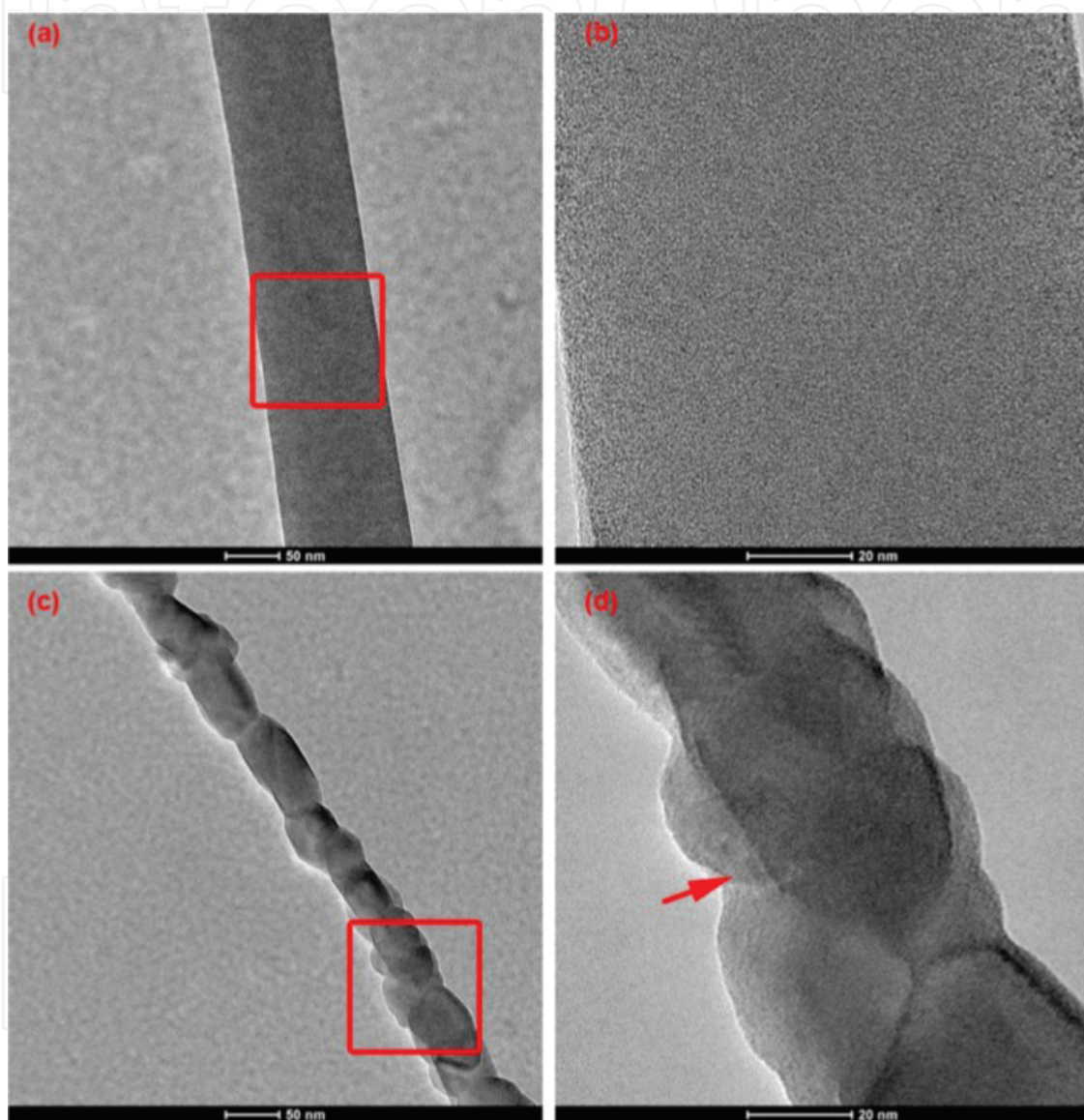

Figure 9. TEM images of the fibres electrospun from the solution of 0.1 M zinc acetate and 0.12 g/mL PVP. After calcination (a, b) at 300°C for 10 min and (c, d) at 500°C for 2 hours [33].

Figure 10 shows the XRD patterns of ZnO-PVP composite nanofibers after calcination at 300°C for 10 minutes and after calcination at 500°C for 2 hours, respectively. The XRD pattern for the sample calcined at 300°C for 10 minutes indicates amorphous ZnO in nature. Characteristic peaks for ZnO are rather weak and obscure, which indicates that only few

portions of crystalline ZnO are present under this calcination condition. Strong diffraction peaks in the pattern come from the substrate used for XRD measurement. As for the sample with calcination at 500 °C for 2 hours, five diffraction peaks at 31.76°, 34.34°, 36.20°, 56.50°, and 62.84° appear corresponding to (100), (002), (101), (110), and (103) of the wurtzite crystal structure, respectively. These diffraction peaks can be indexed to a wurtzite hexagonal phase of ZnO. And the phase of the ZnO nanofibers obtained after calcination at 500°C for 2 hours is rather pure, because no characteristic peaks for other impurities were found in the XRD pattern. So, it can be conclude that the calcination condition plays an important role in crystallizing the as-spun ZnO-PVP nanofibers and removing residual PVP component from the nanofibers.
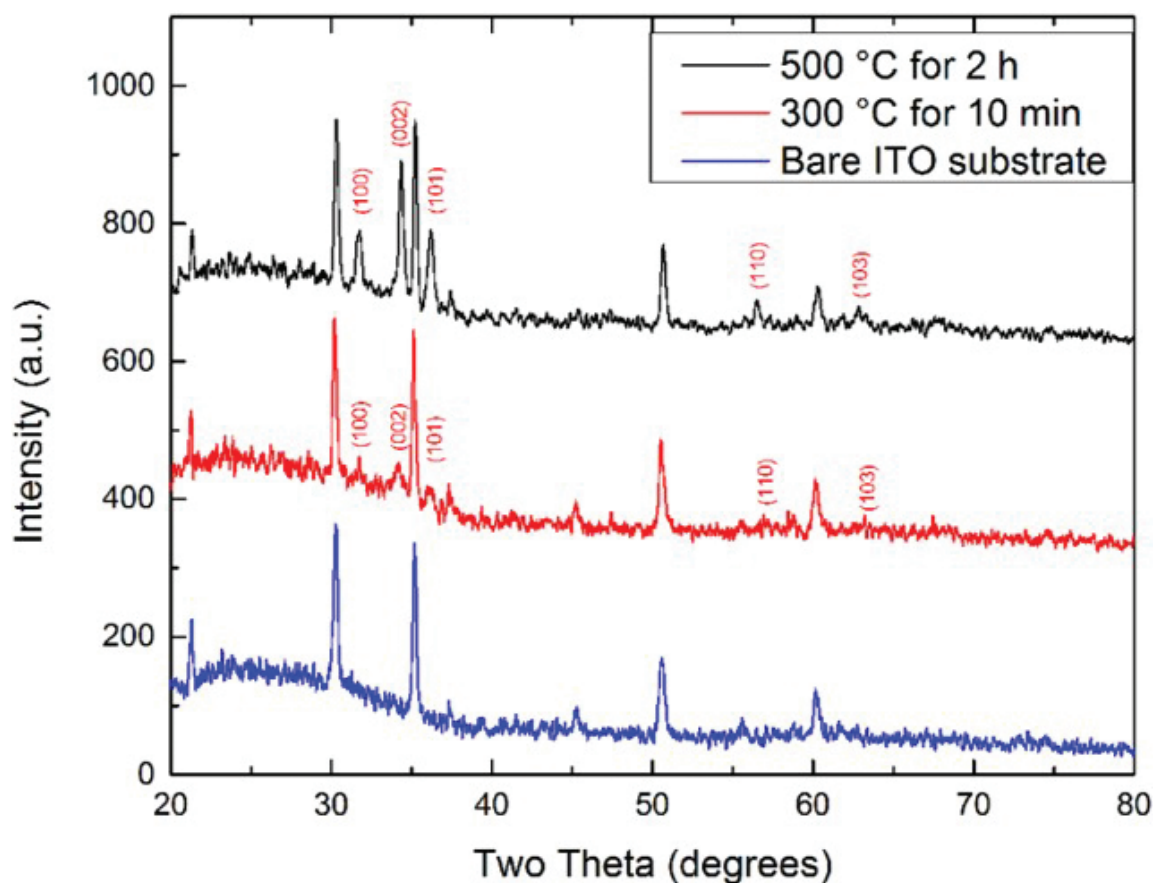

Figure 10. XRD pattern of ZnO nanofibers after calcination under different conditions. The ZnO nanofibers were synthesized using the precursor solution containing 0.1 M zinc acetate and 0.14 g/mL PVP [33].

3. Applications of electrospun nanofibers in the fields of energy

Electrospun nanofibers possess large surface area, high chemical reactivity, and relatively low density, which could contribute a higher absorption of light and dye than the bulk counterparts. These unique optical and electronic properties enable them to be widely applied to a

variety of energy harvesting and storage devices, such as solar cells, photocatalysts, fuel cells, and lithium-ion batteries.

3.1. Solar cell applications

Electrospun nanofibers are commonly made from metal oxides, composites, or surface modification. Metal oxide nanofibers, e.g., ZnO nanofibers and Ti_2O nanofibers, are some of the mostly used nanofibers in solar cell applications. One can archive high power conversion efficiency by fast charge transfer and efficient charge separation introduced by nanofibers. Many polymers, such as PVP, polymethylmethacrylate, and polystyrene, are added into the solution to increase the viscosity for the electrospinning of metal oxide nanofibers. Among these polymers, PVP is the most popular one for its high solubility in various solvents and possibility in mass production [34]. It can used to substitute the liquid state electrolyte for solid or semi-solid electrolyte for dye-sensitized solar cell devices. Hybrid solar cells and dye-sensitized solar cells are two major applications of nanofibers in solar cells, which will be introduced as following.

3.1.1. Hybrid solar cells

Hybrid solar cells have attracted considerable research interest as a promising type of solar cells in which the merits of organic and inorganic materials combine. Commonly used combination of organic and inorganic material in hybrid solar cells is polymers and metal oxides. Both of them play important role in improving the performance of hybrid solar cells [35]. The polymers, e.g., poly(3-hexylthiophene-2,5-diyl) (P3HT) and phenyl-C61-butyric acid methyl ester (PCBM), could constitute a donor-acceptor system just like they work in polymer solar cells. The inorganic materials (e.g., ZnO and Ti_2O) could help improve electron transport for the donor-acceptor system, which is essential for archiving high power conversion efficiency. It has been reported that nanofibers of polymer-metal oxide composites could be fabricated by the electrospinning technique. One-dimensional nanofibrous structure provides much larger interface than the conventional planar structure of polymers and metal oxides. Researcher recently found that the usage of metal oxide nanofibers in hybrid solar cells could not only increase the interfacial area but also contribute to the improvement of electron mobility and the dissociation of excitons. The external quantum efficiency could be improved tremendously at the absorption peak of P3HT due to the enhanced dissociation of photo-generated excitons when an electrospun ZnO nanofiber layer is inserted into the P3HT:PCBM blend. Hybrid solar cells using ZnO nanofibers and a P3HT:PCBM donor-acceptor system could yield a power conversion efficiency over 2% [36].

Our group has worked on hybrid solar cells using ZnO nanofibers as electron transport materials. **Figure 11** presents a scheme for the structure of devices used. ZnO nanofibers were fabricated as described in previous section. A blend of P3HT:PCBM is added into the ZnO nanofiber mat. To avoid direct contact between the P3HT:PCBM blend layer and the indium tin oxide (ITO) electrode, a thin ZnO layer was spin coated on the ITO-coated glass substrate before electrospinning of ZnO nanofibers. Here, MoO_x was used as the anode interfacial layer

instead of commonly used mixture of poly(3,4-ethylenedioxythiophene) and polystyrene sulfonate, because it has higher charge extraction efficiency.
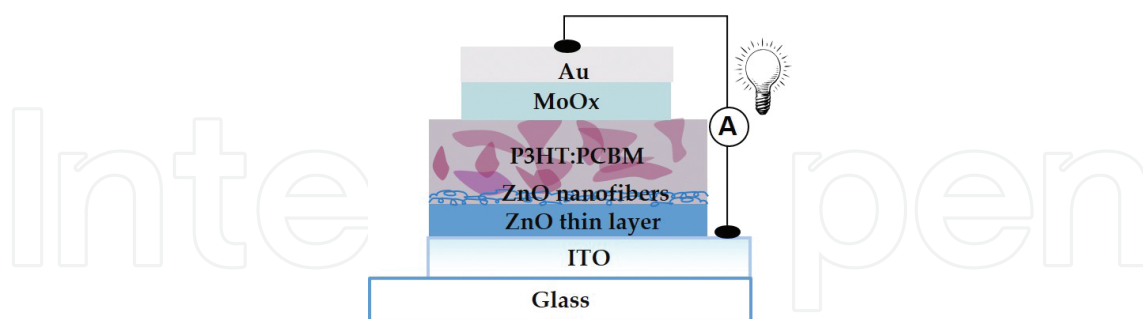

Figure 11. Device structure of hybrid solar cells using ZnO nanofibers as an electron-transporting layer.

To crystallize the electrospun ZnO nanofibers, calcinations at 300 and 500°C were performed. The nanoscale surface morphologies of calcined ZnO nanofibers were investigated by atomic force microscopy (AFM). As shown in **Figure 12**, ZnO nanofibers can be identified from the surface of ITO substrate after calcination. As the calcination temperature increases from 300 to 500°C, more particles can be observed. As confirmed by TEM and XRD (see **Figures 9** and
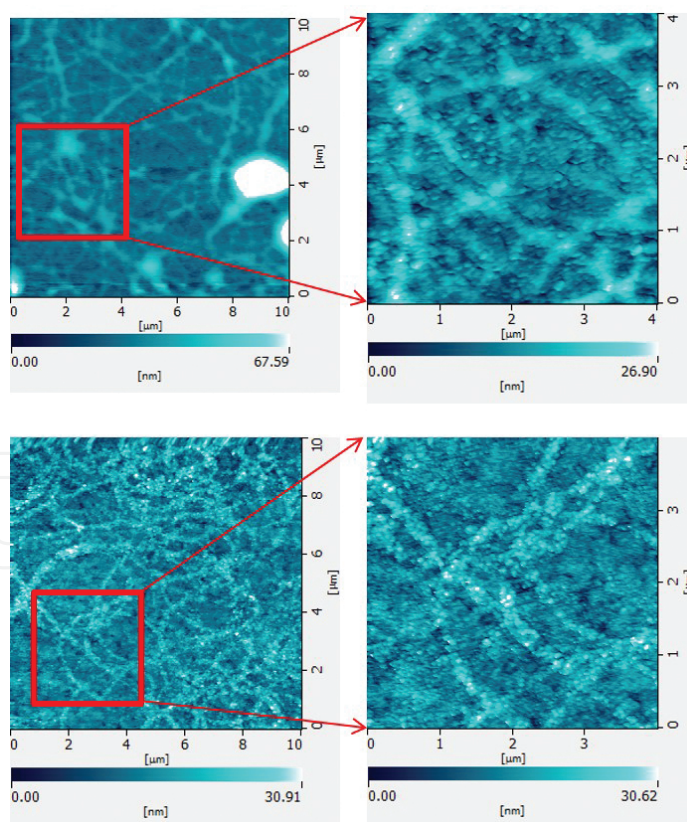

Figure 12. AFM topographies of ZnO nanofibers after calcination at 300°C for 10 min (top) and at 500°C for 2 hours (bottom).

10), these particles are crystalline ZnO. From the magnified AFM images in **Figure 12**, one can also find that the PVP component on the surface of the nanofibers was partially removed after calcination at 500°C. The surface of ZnO nanofibers, however, could still be compositionally rich in PVP even after calcination. The residual PVP may create a contact barrier between the ZnO nanofibers and the P3HT:PCBM blend resulting in a low charge collection efficiency.

Previous paper has shown that the PVP on the surface of colloidal surface could be removed by UV-ozone treatment [37, 38]. To ensure a good contact between ZnO nanofibers and the active layer, we performed UV-ozone treatment on ZnO nanofibers to remove residual PVP from the nanofibers. The atomic concentration of zinc, carbon, and oxygen in the UV-ozone–treated ZnO nanofibers based on the Zn *2p*, C *1s*, and O *1s* XPS spectra is summarized in **Figure 13**. The atomic concentration of zinc and oxygen present in the UV-ozone–treated ZnO nanofibers both increase as the time of treatment. The atomic concentration of oxygen shows relatively larger increment than zinc because there is a competition between increment and decrement in the oxygen atomic concentration by UV-ozone treatment and removal of PVP, respectively. On the contrary, the atomic concentration of carbon from the PVP in the ZnO nanofibers reduced by the UV-ozone treatment, especially from 5 to 7.5 min.
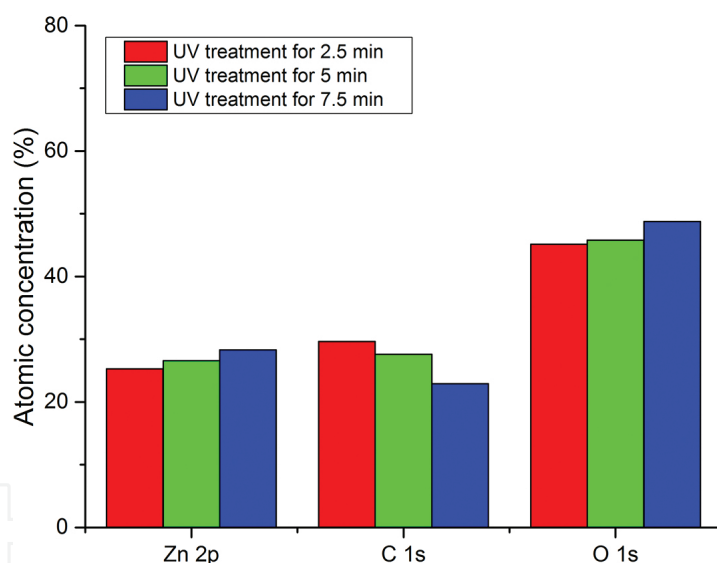

Figure 13. Atomic concentrations of zinc, carbon, and oxygen based on the corresponding XPS spectra. The ZnO nanofibers were measured after UV-ozone treatment for 2.5, 5, and 7.5 min.

The performance result for the hybrid solar cells with UV-ozone–treated ZnO nanofibers is shown in **Figure 14**. The J-V characteristics for the hybrid solar cells were measured under AM 1.5G solar illumination at 100 mW cm^{-2}. The ZnO nanofibers were UV-ozone treated for 2.5, 5, and 7.5 min, resulting in a variation in the J$_{sc}$. Although the J$_{sc}$ decreases from 2.5 to 5 min, it increases a lot at 7.5 min. As for the UV-ozone treatment for a longer time, it may reduce the electron extraction efficiency due to excess oxygen on the surface of the ZnO nanofibers. It is worth noting that UV-ozone treatment could somewhat contribute to an improvement of charge collection but the power conversion efficiency of the hybrid solar cells with UV-ozone–

treated ZnO nanofibers is lower than the reference device. Various chemical surface treatments are investigated for the application of ZnO nanofibers in hybrid solar cells.
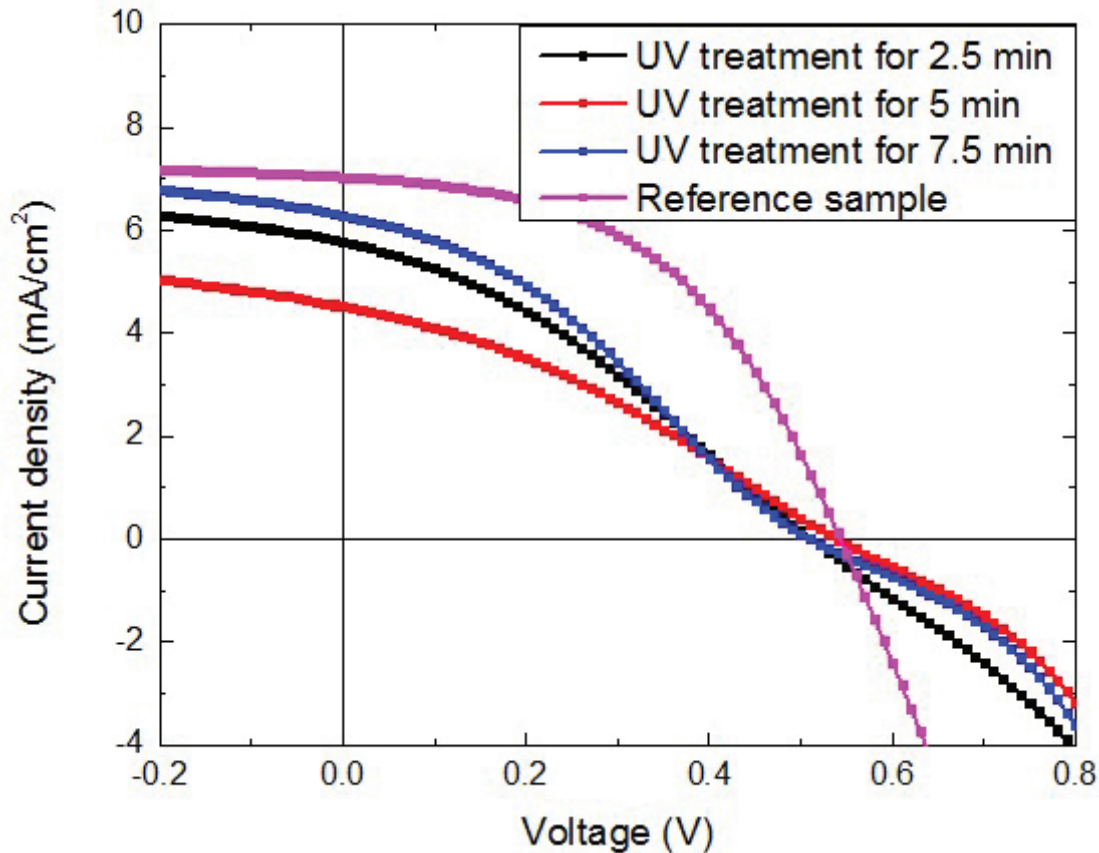

Figure 14. J-V characteristics for hybrid solar cells with UV-ozone–treated ZnO nanofibers for various treatment times (2.5, 5, and 7.5 min).

PVP can dissolve in water and a lot of polar solvents. Here, we use the solubility of PVP in ethanol, acetone, and isopropyl alcohol (IPA) to treat the ZnO nanofibers and remove the residual PVP in the nanofibers. The J-V characteristics for the hybrid solar cells with surface-treated ZnO nanofibers are shown in **Figure 15**. Corresponding performance parameters are presented in **Table 1**. The J_{sc} of the solar cell decreases dramatically after immersing the ZnO nanofibers into an ethanol solution. This effect is aggravated by an ultrasonic cleaning, which results in a smaller fill factor of 0.27 compared to the immersed device. While the treatment with acetone and IPA exhibits positive effect. After ultrasonic cleaning in acetone and IPA subsequently for 1 min, the open voltage of the solar cells increases from 0.54 to 0.61 V. It implies that the ZnO nanofibers have more contact with the active layer. The contact quality between the electron transport layer like ZnO nanofibers and the active layer like the P3HT:PCBM blend layer can be reflected by the values of shunt resistance (R_{sh}) and series resistance (R_s). Researchers found that contact resistance and charge recombination at the interface are major reasons for giving rise to the increase in R_s and the drop in R_{sh}, respectively [39]. A low R_s of 14 Ω cm^2 and a high R_{sh} of 952 Ω cm^2 strongly support the assertion that

ultrasonic cleaning in acetone and IPA could effectively remove the residual PVP from the ZnO nanofibers and ensure a good contact between the ZnO nanofibers and the P3HT:PCBM layer.
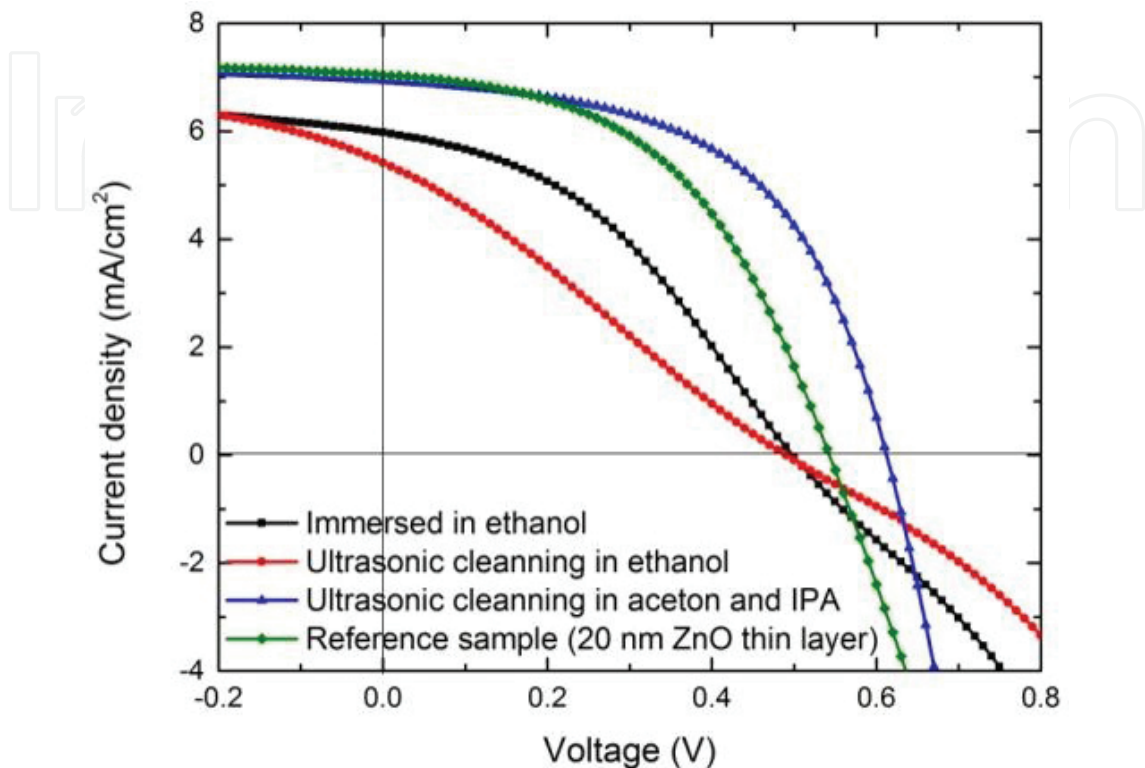

Figure 15. J-V characteristics for hybrid solar cells with ZnO nanofibers after different surface treatment.

Device	Surface treatment method	PCE [%]	V_{oc} [V]	J_{sc} [mA/cm²]	FF	R_{sh} [Ω cm²]	R_s [Ω cm²]
A	Immersed in ethanol	1.18	0.50	5.98	0.40	500	53
B	Ultrasonic cleaning in ethanol	0.72	0.49	5.42	0.27	145	106
C	Ultrasonic cleaning in acetone and IPA	2.31	0.61	6.93	0.54	952	18
D	20 nm ZnO thin layer with no treatment	1.87	0.54	7.04	0.49	869	25

Table 1. Averaged solar cell performance of the hybrid solar cells with surface-treated ZnO nanofibers as electron transport media. PCE: power conversion efficacy; V_{oc}: open-circuit voltage; J_{sc}: short-circuit current; FF: fill factor; R_{sh}: shunt resistance; R_s: series resistance.

Although electrospun nanofibers show great potential in hybrid solar cells applications, there are still some problems to be solved. (1) Removing residual polymers. The polymers using for fabricating metal oxide nanofibers should be removed before applied to hybrid solar cells. Only calcination cannot remove completely the residual polymers, which limits the function of metal oxide nanofibers. (2) Reducing the diameter of nanofibers and spacing to around 10 nm. As we discussed in Section 2.2, the diameter of electrospun metal oxide nanofibers is

usually in the range of several tens of nanometers (30 nm to several micrometres in case of electrospun ZnO nanofibers), which is still above the diffusion length of exciton. The diffusion length of excitons in electronic devices like solar cells is usually around 10 nm. Hence, electrospun metal oxide nanofibers with finer size are expected to get improved excition dissociation and higher power conversion efficiency. (3) Controlling the orientation of nanofibers. Vertically aligned metal oxides could provide an ideal structure for suppressing of the recombination of dissociated electrons and holes. But most of the orientations of electrospun nanofibers are parallel to the substrate. Vertically aligned electrospun nanofibers have addressed seldom until now. Control of orientation, particularly vertical orientation, is still a challenge for the hybrid solar cell application of electrospun nanofibers. In general, the possibility to control the purity, diameter, spacing, and orientation on metal oxide nanofibers is a critical issue for all researchers.

3.1.2. Dye-sensitized solar cells

Dye-sensitized solar cells usually exploit porous structure of metal oxide nanoparticles to absorb sensitizing dyes, see **Figure 16**. The usage of particles, however, could result in charge-carrier recombination and low power conversion efficiency, because the conduction of electrons in the matrix of nanoparticles could be diminished across the boundaries of the metal oxide nanoparticles.
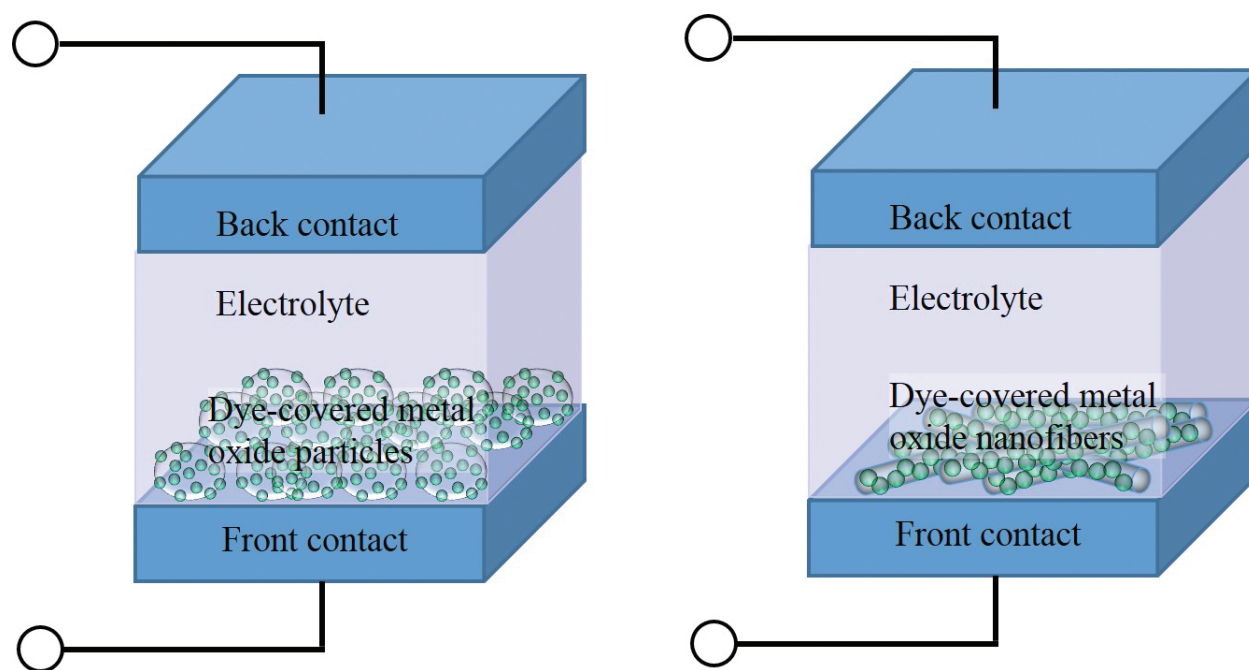

Figure 16. A scheme for dye-sensitized solar cells with dye-covered metal oxide particles (left) and dye-covered metal oxide nanofibers (right).

Comparing with sintered nanoparticles, one-dimensional metal oxide nanofibers can produce high charge conduction because they have smaller particle boundaries and higher specific surface area (see **Figure 16**), which can absorb more sensitizing dyes [40]. The size of the pores

in electrospun metal oxide nanofibers is usually larger than that in metal oxide nanoparticles, which facilitates the filling of viscous electrolyte into nanofibers. It has been demonstrated that dye-sensitized solar cells using electrospun TiO_2 nanofibers as electrode could reach power conversion efficiency comparable with that produced by liquid electrolyte system [41]. However, there are problems when applying electrospun mental oxide nanofibers to dye-sensitized solar cells. The porous metal oxide electrodes have poor adhesion to the substrate after removing the polymer component through calcination at high temperature. As shown in **Figure 9**, the metal oxide nanofibers shrink prominently after calcination because of the large stress generated at high temperature. The shrinkage in calcination could affect tremendously not only dye-sensitized solar cell devices but also other energy applications of metal oxide nanofibers. More details about the effect on hybrid solar cell devices are given later. A variety of methods have been reported to solve the adhesion problem for metal oxide nanofibers. Some researchers use pretreatment or solvent vapour to diminish the stress effect during calcination and improve the adhesion between metal oxide nanofibers and the substrate [42].

3.2. Lithium-ion battery applications

Lithium-ion batteries have attracted considerable attention in both research and industrial development due to their advantages, such as high energy density, long cycle life, low gravimetric density, and flexible design. Rechargeable solid lithium-ion batteries have been widely applied to portable electronic devices for more than 25 years. The solid lithium-ion batteries produce electrical energy by converting chemical energy via redox reactions at the electrode. Similarly to working mechanism of fuel cells, lithium-ion batteries comprise an electrolyte sandwiched by an anode and a cathode. The electrolyte is an insulator for electrons but a conductor for Li^+. Carbon/graphite is commonly used anode material for conventional batteries. A lithium-metal oxide (e.g., $LiCoO_2$, $LiMn_2O_4$, and $LiNiO_2$) is usually selected as the cathode materials. And the organic electrolyte could be lithium hexafluorophosphate ($LiPF_6$) salt.

As the demand for energy increases, lithium-ion batteries are expected to be applied to more applications requiring fast charging and discharging at high power rates like electric vehicles. So, many improvements, for instance, cycling life, charge/discharge rate, power, energy density, are needed to meet the requirements. Researchers have developed various novel materials and nanostructures for both electrodes and electrolytes of lithium-ion batteries. Electrospun nanofibers is one of the most promising structures for high-performance lithium-ion batteries due to their one-dimensional structure and low manufacturing cost. $LiCoO_2$ nanofibers have been used as the cathode of lithium-ion battery to get a fast solid state diffusion [43]. While the electrospun $LiCoO_2$ nanofibers have a large loss in capacity during the charge-discharge process, resulting from the dissolution of cobalt and lithium cations forming Li_2CO_3 and CoF_2 impurities. To increase stability and cycling performance of lithium-ion batteries, coatings on the electrospun nanofibers have also been investigated. Besides cathode materials, electrospun nanofibers have been employed for use as anode and electrolyte.

3.3. Other applications

Electrospun metal oxide nanofibers can also be applied to other devices, such as fuel cells, supercapacitors, and so on. For example, many electrospun metal oxide (e.g., TiO_x, MnO_x, WO_x, and SnO_2) nanofibers can be used as catalyst support in fuel cells.

4. Conclusions

The diameter of electrospun metal oxide nanofibers can be controlled by adjusting the properties of the solution. Ultrathin nanofibers formed when using very dilute solution. But fabrication of metal oxide nanofibers at the scale of 10 nm or smaller is still a challenge. Calcination process after electrospinning determined the chemical composition and crystallization of resultant nanofibers. It could help crystallize metal oxide nanofibers, but somewhat limit the practical application of electrospun nanofibers due to the high temperature. Residual polymers in the calcined metal oxide nanofibers could be removed by chemical surface treatments. After surface treatment, the nanofibers have more contact with the active layer, which contributes high performance for solar cells.

Acknowledgements

Author details

Yingjie Liao[1*], Takeshi Fukuda[2] and Suxiao Wang[3]

*Address all correspondence to: ajiewy@gmail.com

1 Centre de Recherches sur les Macromolécules Végétales (CERMAV, UPR-CNRS 5301) affiliated with Grenoble Alpes University, Grenoble, France

2 Department of Functional Materials Science, Saitama University, Saitama, Japan

3 Shanghai Aircraft Design and Research Institute, Shanghai, China

References

[1] Serp P, Corrias M, Kalck P. Carbon nanotubes and nanofibers in catalysis. Appl Catal A-Gen. 2003;253(2):337–58.

[2] Lu XF, Zhang WJ, Wang C, Wen TC, Wei Y. One-dimensional conducting polymer nanocomposites: synthesis, properties and applications. Prog Polym Sci. 2011;36(5): 671–712.

[3] De Jong KP, Geus JW. Carbon nanofibers: catalytic synthesis and applications. Catal Rev-Sci Eng. 2000;42(4):481–510.

[4] Yoshimoto H, Shin YM, Terai H, Vacanti JP. A biodegradable nanofiber scaffold by electrospinning and its potential for bone tissue engineering. Biomaterials. 2003;24(12): 2077–82.

[5] Yang F, Murugan R, Wang S, Ramakrishna S. Electrospinning of nano/micro scale poly(L-lactic acid) aligned fibers and their potential in neural tissue engineering. Biomaterials. 2005;26(15):2603–10.

[6] Sill TJ, von Recum HA. Electro spinning: applications in drug delivery and tissue engineering. Biomaterials. 2008;29(13):1989–2006.

[7] Pham QP, Sharma U, Mikos AG. Electrospinning of polymeric nanofibers for tissue engineering applications: a review. Tissue Engineering. 2006;12(5):1197–211.

[8] Gopal R, Kaur S, Ma ZW, Chan C, Ramakrishna S, Matsuura T. Electrospun nanofibrous filtration membrane. J Membr Sci. 2006;281(1–2):581–6.

[9] Gibson P, Schreuder-Gibson H, Rivin D. Transport properties of porous membranes based on electrospun nanofibers. Colloids Surf A: Physicochem Eng Aspects 2001;187:469–81.

[10] Barhate RS, Ramakrishna S. Nanofibrous filtering media: filtration problems and solutions from tiny materials. J Membr Sci. 2007;296(1–2):1–8.

[11] Liang D, Hsiao BS, Chu B. Functional electrospun nanofibrous scaffolds for biomedical applications. Adv Drug Delivery Rev. 2007;59(14):1392–412.

[12] Burger C, Hsiao BS, Chu B. Nanofibrous materials and their applications. Annu Rev Mater Res. 2006; 36:333–68.

[13] Zong XH, Kim K, Fang DF, Ran SF, Hsiao BS, Chu B. Structure and process relationship of electrospun bioabsorbable nanofiber membranes. Polymer. 2002;43(16):4403–12.

[14] Virji S, Huang JX, Kaner RB, Weiller BH. Polyaniline nanofiber gas sensors: examination of response mechanisms. Nano Lett. 2004;4(3):491–6.

[15] Liu HQ, Kameoka J, Czaplewski DA, Craighead HG. Polymeric nanowire chemical sensor. Nano Lett. 2004;4(4):671–5.

[16] Huang JX, Virji S, Weiller BH, Kaner RB. Polyaniline nanofibers: facile synthesis and chemical sensors. J Am Chem Soc. 2003;125(2):314–5.

[17] Wu Q, Xu YX, Yao ZY, Liu AR, Shi GQ. Supercapacitors based on flexible graphene/polyaniline nanofiber composite films. ACS Nano. 2010;4(4):1963–70.

[18] Ramakrishna S, Fujihara K, Teo WE, Yong T, Ma ZW, Ramaseshan R. Electrospun nanofibers: solving global issues. Mater Today. 2006;9(3):40–50.

[19] Antolini E. Carbon supports for low-temperature fuel cell catalysts. Appl Catal B: Environ. 2009;88(1–2):1–24.

[20] Wu H, Zhang R, Liu XX, Lin DD, Pan W. Electrospinning of Fe, Co, and Ni nanofibers: synthesis, assembly, and magnetic properties. Chem Mater. 2007;19(14):3506–11.

[21] Li D, Herricks T, Xia YN. Magnetic nanofibers of nickel ferrite prepared by electrospinning. Appl Phys Lett. 2003;83(22):4586–8.

[22] Jose R, Thavasi V, Ramakrishna S. Metal oxides for dye-sensitized solar cells. J Am Ceram Soc. 2009;92(2):289–301.

[23] Antolini E, Gonzalez ER. Ceramic materials as supports for low-temperature fuel cell catalysts. Solid State Ionics. 2009;180(9–10):746–63.

[24] Agarwal S, Greiner A, Wendorff JH. Functional materials by electrospinning of polymers. Prog Polym Sci. 2013;38(6):963–91.

[25] Lakshmi BB, Patrissi CJ, Martin CR. Sol–gel template synthesis of semiconductor oxide micro- and nanostructures. Chem Mater. 1997;9(11):2544–50.

[26] Hartgerink JD, Beniash E, Stupp SI. Self-assembly and mineralization of peptide-amphiphile nanofibers. Science. 2001;294(5547):1684–8.

[27] Li D, Xia YN. Electrospinning of nanofibers: reinventing the wheel? Adv Mater (Weinheim, Germany). 2004;16(14):1151–70.

[28] Lee MR, Eckert RD, Forberich K, Dennler G, Brabec CJ, Gaudiana RA. Solar power wires based on organic photovoltaic materials. Science. 2009;324(5924):232–5.

[29] Huynh WU, Peng XG, Alivisatos AP. CdSe nanocrystal rods/poly(3-hexylthiophene) composite photovoltaic devices. Adv Mater (Weinheim, Germany). 1999;11(11):923–927.

[30] Fan X, Chu ZZ, Wang FZ, Zhang C, Chen L, Tang YW, et al. Wire-shaped flexible dye-sensitized solar cells. Adv Mater (Weinheim, Germany). 2008;20(3):592–595.

[31] Bessel CA, Laubernds K, Rodriguez NM, Baker RTK. Graphite nanofibers as an electrode for fuel cell applications. J Phys Chem B. 2001;105(6):1115–8.

[32] Thavasi V, Singh G, Ramakrishna S. Electrospun nanofibers in energy and environmental applications. Energy Environ Sci. 2008;1(2):205–21.

[33] Liao Y, Fukuda T, Kamata N, Tokunaga M. Diameter control of ultrathin zinc oxide nanofibers synthesized by electrospinning. Nano Res Lett. 2014;9:267.

[34] Zhang X, Thavasi V, Mhaisalkar SG, Ramakrishna S. Novel hollow mesoporous 1D TiO2 nanofibers as photovoltaic and photocatalytic materials. Nanoscale. 2012;4(5): 1707–16.

[35] Gonzalez-Valls I, Lira-Cantu M. Vertically-aligned nanostructures of ZnO for excitonic solar cells: a review. Energy Environ Sci. 2009;2(1):19–34.

[36] Olson DC, Piris J, Collins RT, Shaheen SE, Ginley DS. Hybrid photovoltaic devices of polymer and ZnO nanofiber composites. Thin Solid Films. 2006;496(1):26–9.

[37] Aliaga C, Park JY, Yamada Y, Lee HS, Tsung C-K, Yang P, et al. Sum frequency generation and catalytic reaction studies of the removal of organic capping agents from Pt nanoparticles by UV–ozone treatment. J Phys Chem C. 2009;113(15):6150–5.

[38] Small CE, Chen S, Subbiah J, Amb CM, Tsang SW, Lai TH, et al. High-efficiency inverted dithienogermole-thienopyrrolodione-based polymer solar cells. Nat Photonics. 2012;6(2):115–20.

[39] Liang ZQ, Zhang QF, Wiranwetchayan O, Xi JT, Yang Z, Park K, et al. Effects of the morphology of a ZnO buffer layer on the photovoltaic performance of inverted polymer solar cells. Adv Funct Mater. 2012;22(10):2194–201.

[40] Onozuka K, Ding B, Tsuge Y, Naka T, Yamazaki M, Sugi S, et al. Electrospinning processed nanofibrous TiO2 membranes for photovoltaic applications. Nanotechnology. 2006;17(4):1026–31.

[41] Song MY, Kim DK, Jo SM, Kim DY. Enhancement of the photocurrent generation in dye-sensitized solar cell based on electrospun TiO2 electrode by surface treatment. Synth Met. 2005;155(3):635–8.

[42] Fujihara K, Kumar A, Jose R, Ramakrishna S, Uchida S. Spray deposition of electrospun TiO 2 nanorods for dye-sensitized solar cell. Nanotechnology. 2007;18(36):365709.

[43] Gu Y, Chen D, Jiao X. Synthesis and electrochemical properties of nanostructured LiCoO2 fibers as cathode materials for lithium-ion batteries. J Phys Chem B. 2005;109(38):17901–6.